coesite. I, therefore, concluded that the possibility of carbon diffusion into the sample must be eliminated in some way, since otherwise the interaction of carbon and quartz complicates the picture too much. The next step involved taking a platinum capsule. Then I slightly raised the pressure and the temperature. In a new series of experiments, the coesite yield was nearly 100%. In what follows we carry out the experiments under the highest pressure possible and a temperature of 1800–2000 °C. The result was again coesite, but there was also a significant difference in the outcome. An unknown phase with a high refractive index and high birefringence appeared systematically. This phase either covered the coesite or formed laminated and needle-shaped grains. We named this phase in the laboratory record as 'phase X'. Phase X emerged only as an impurity, maybe because there was never enough time for it to form in abundance. So the next time the experiment was prolonged to three hours. The result was an explosion. Another prolonged experiment, and another explosion. This prompted to use water jackets to cool the steel exteriors of the chamber. So then the first experiment with jackets. The pressure was higher as before than the last transition point in bismuth and the heater's output power corresponded to a temperature of about 2000 °C. The experiment was continued for two hours, and the chamber was not fractured. Finally I took out the platinum capsule and noticed certain difference. Before it was sufficient to break off the lid of the capsule, and the contents could easily be poured out, with the walls of the capsule remaining clean. Now, however, the capsule's lids could be separated from the capsules only together with a fraction of the contents. The material taken from the center of the capsule was practically pure coesite. Then I noticed phase X, and the quantity of it was slightly greater. The second and third experiments followed in the course of one weak. The result was the same. I still ignored the material stuck to the capsule's lids.

Next I reduced the output power of the heater and carried out further experiments. I extracted the 'lentil' and took out the capsule. And what did I find? I found that it was impossible to open the capsule. The lid had stuck. It was proved to be impossible to break off the side surface of the capsule. Finally I had to use clippers and cut the capsule open. I took some of the substance and placed it on the microscope slide. The substance was neither quartz nor coesite. What I saw was an unknown fibrous material with a high refractive index. Of course this was phase X, but it was not easily recognizable in such large quantities. There were a few needle-shaped formations and even well-formed elongated crystals. Some of the crystals appeared to be green in crossed Nicol prisms. The birefringence of the material was high. Then I began to suspect dimly what had happened: the jackets with running water intensified the removal of heat, so that the temperature in the chamber fell, and we 'landed' into the stability region of the new phase. Analytical chemistry techniques were then employed for purposes establishing whether all the effect was not the result of contamination. There were fears that, possibly, graphite diffuses into the capsule and interacts with silica, with the result that some carbon compounds are formed, etc. After checking and rechecking, hesitating and thoroughly discussing the results, it was confirmed that a new dense phase of silica had been discovered. Finally, a paper was written and submitted to publication. I have left out many details that made research more complicated since they are of no interest now.

In August 1961, the paper was published and received much attention. And then, in December 1961, I received a letter from Edward Chao in which he reported about the discovery of a new mineral, a natural analog of the phase X, at Meteor Crater in Arizona. Chao also wrote that the new mineral was named stishovite.

Strictly speaking the scientific story of the discovery ended with these events. What followed is quite a different story...

PACS number: 81.30.Hd
DOI: 10.1070/PU2002v045n04ABEH001155

Stishovite and its implications in geophysics: new results from shock-wave experiments and theoretical modeling

S-N Luo, J Mosenfelder, P Asimow, T J Ahrens

1. Introduction

Pure stishovite and coesite samples with densities of 4.31 ± 0.04 and 2.92 ± 0.03 g/cm^3, respectively, and dimensions appropriate for planar shock-wave experiments have been synthesized with a multianvil high-pressure press. The principal Hugoniot centered at stishovite obtained by shock loading up to 235 GPa yields a linear shock velocity (U_s)–particle velocity (u_p) relationship $U_s = C_0 + su_p$, where $C_0 = 9.08$ km/s, and $s = 1.23$. The new shock-wave data for coesite to 140 GPa agree with, and extend, the former study. These data along with previous studies on other polymorphs now provide Hugoniots for the major polymorphs of SiO_2 (fused quartz, quartz, coesite and stishovite). The Grüneisen parameter for stishovite under compression obtained from the internal energy and pressure differences between different principal Hugoniots of silica polymorphs is $\gamma = 1.35(V/V_0)^q$, where $q = 2.6 \pm 0.2$. Previously melting of stishovite at 70 and 113 GPa was inferred from shock temperature measurements. These are in accord with recent molecular dynamics modeling of the high-pressure fusion curve of stishovite.

Silica is important not only as the main constituent of the Earth and other terrestrial planets but also as a model system to study the fundamental physics of material properties, such as polymorphic phase changes and interatomic potentials [1]. To understand the seismic structure of the Earth and transport processes (e.g., heat and mass), knowledge of thermodynamics of the $MgO-SiO_2$ system is crucial. Free silica may exist as stishovite (or post-stishovite phases) in the Earth from 300 km depth (10 GPa) in the upper mantle to 2891 km at the core-mantle boundary (CMB, 136 GPa). Stishovite-type phases may play a key role in chemical reactions in the lowermost mantle [1–3]:

$$\begin{aligned}&(Mg_{0.9}Fe_{0.1})\,SiO_3\,(\text{perovskite}) + 0.15Fe_{0.9}(\text{liquid})\\&\quad\leftrightarrow 0.9MgSiO_3(\text{perovskite}) + 0.2FeO(\text{hpp})\\&\quad + 0.05FeSi(\text{liquid}) + 0.05SiO_2(\text{stishovite})\,,\end{aligned} \tag{1}$$

$$\begin{aligned}&(Mg,\,Fe)O(B1) + SiO_2(\text{stishovite})\\&\qquad\leftrightarrow (Mg,Fe)SiO_3(\text{perovskite}).\end{aligned} \tag{2}$$

These reactions sequester iron from the mantle into the metallic core and consume silica into Mg-perovskite and

may have occurred during the early accretion history of the Earth [3]. In this sense free silica might be scarce at the lower mantle. Stishovite was the first silicate discovered with Si^{4+} octahedral coordination with O^{2-}, characteristic of all the lower mantle silicate phases, and the elastic, thermodynamic and transport properties of stishovite in joint presence with other materials remain important for seismic and geodynamic studies of the Earth. Stishovite and post-stishovite phases are also important for planetary impact processes: the structure of shocked SiO_2-bearing rocks and meteorites constrains the interpretation of impact process [4, 5].

Extensive and detailed studies on the silica system have been conducted for long time with various techniques [1]. For shock wave experiments, McQueen et al. [6] reanalyzed the first shock-wave studies on fused quartz and quartz by Wackerle [7] and demonstrated that the high-pressure region above 30 GPa for both initially crystal quartz and fused quartz appeared to behave as if transition to the recently discovered rutile phase had occurred. They predicted $C_0 = 10.0$ km/s and $s = 1.0$ for stishovite Hugoniot. Additional studies such as those by Fowles [8], Ahrens and Rosenberg [9] and some Russian studies (see Trunin [10] and references cited therein for a complete review) on crystal and porous quartz, fused silica, crystabolite and coesite all demonstrated transition to stishovite as suggested by McQueen et al. [6]. Podurets et al. [11] proposed the stishovite Hugoniot as $C_0 = 7.6$ km/s and $s = 1.41$, based on their shock-wave experiments. Furnish and Ito [12] had synthesized polycrystalline stishovite for shock-wave measurements. Unfortunately, their samples were heterogeneous. They varied in both porosity and stishovite content such that the initial bulk densities varied from 3.8 to 4.07 g/cm^3. This gave rise to considerable scatter in the resulting data. Although the shock-compressed states are undeniably compressed stishovite, the data are too scattered to provide an independent contribution to our knowledge of the equation of state of this phase. The direct measurement of the Hugoniot of stishovite is of paramount importance as suggested by Trunin [10].

Advances in static synthesis techniques, shock-wave diagnostics and theoretical modeling enable further study on high-pressure silica phases [13, 14]. To address the equation of state and the post-stishovite transition along the Hugoniot [10], direct shock-wave loading of stishovite is realized by the synthesis of pure stishovite samples with dimensions circumventing edge effects and ensuring high accuracy of measurement in planar impact experiments [13]. The melting point of stishovite at 70 and 113 GPa was previously inferred from shock-induced melting experiments [15]. New molecular dynamics modeling of stishovite melting [14] complements the shock-wave study. In this review, we summarize our experimental work on high-pressure phases of silica and theoretical study on the phase diagram of stishovite.

2. Static synthesis and dynamic loading of coesite and stishovite

To conduct planar shock-wave loading on a light gas gun, the diameter to thickness ratio of the sample should be larger than 3 to avoid edge effects. The accuracy of the present shock-wave velocity measurement (± 1 ns) is limited by the streak camera capable of measuring 80 – 100 ns propagation time in a 1 mm thick stishovite or coesite sample. This presents a challenge for the synthesis of stishovite with multianvil high-pressure press: the minimum required dimensions are 3 mm in diameter and 1 mm in thickness. Previously typical dimensions of the recovered sample in laboratory multianvil cells that reach 10 GPa are ~ 1.5 mm in diameter [16]. A new technique was adopted to radically simplify the assembly to maximize space, at the expense of exact characterization of the sample environment [13]. In the synthesis experiments, success is justified by the recovered phase, and precise pressure (P) and temperature (T) control is not important. For this reason, the ZrO_2 insulator, $LaCrO_3$ heater, MgO spacer, and Pt capsule typically used in modern multianvil experiments [16] were dispensed with and only a Re foil was used as both heating element and sample container. The stishovite samples were synthesized using 14-mm sintered MgO octahedra, 8-mm truncation-edge-length carbide anvils and pyrophyllite gaskets. The temperature is monitored with W/Re thermocouple, and pressure is calculated from the loading calibration. The starting material is a cylinder of pure silica glass. Stishovite samples have been synthesized at 14 GPa and 1000 °C, with bulk density of 4.31 ± 0.04 g/cm^3, diameter of about 4 mm, and thickness of about 25 mm. The density was measured using Archimedean method with toluene as the immersion liquid, and quartz as a calibration standard. These samples are pure stishovite with zero porosity as evidenced by optical microscopy and X-ray diffraction (XRD) patterns [13].

Coesite samples have been synthesized with the cubic module in the multianvil press at approximately 4 GPa and 900 °C. The pressure medium is a 21-mm pyrophyllite cube with a barium carbonate sleeve surrounding the graphite heater. The square anvil truncations are 16 mm along each edge. The starting material is silica glass. The final products have bulk densities of 2.92 ± 0.03 g/cm^3 and XRD patterns with only coesite peaks. The coesite samples are ~ 5.3 mm in diameter, and ~ 5 mm in length.

The synthesized coesite and stishovite samples are sectioned into disks and polished for shock-wave experiments. The stishovite and coesite samples mounted in the target assembly have diameter/thickness ratios of approximatily 4 and 5, respectively. Coesite and stishovite samples were mounted in the same target assembly when possible. Planar impact experiments have been conducted on the Caltech two-stage light gas gun with a streak camera measuring the shock velocity, and flash X-ray diagnostics the projectile velocity [13]. By varying the flyer – driver material and projectile velocity, different final states were achieved in the shocked coesite and stishovite samples. The directly measured projectile velocity and shock velocity (U_s) were reduced to shock-state particle velocity (u_p), pressure (P) and specific volume (V) in the sample by the impedance match method [17]. Figure 1 shows the $U_s - u_p$ relationships for stishovite and coesite. The new coesite data are in agreement with Podurets et al. [11] A linear fit to both coesite data sets in stishovite regime gives

$$U_s \ (\mathrm{km\ s^{-1}}) = 2.52 + 1.70\, u_p; \quad \rho_0 = (2.92 \pm 0.03)\ \mathrm{g\,cm^{-3}}. \tag{3}$$

A linear fit to the stishovite data yields

$$U_s \ (\mathrm{km\ s^{-1}}) = 9.08 + 1.23\, u_p; \quad \rho_0 = (4.31 \pm 0.04)\ \mathrm{g\,cm^{-3}}. \tag{4}$$

The corresponding Hugoniot in the $P-V$ plane for stishovite is shown in Fig. 2 along with diamond-anvil cell (DAC) data at low pressures. The stishovite fit to the Vinet universal equation of state [18] yields $K_0 = 326 \pm 4$ GPa and

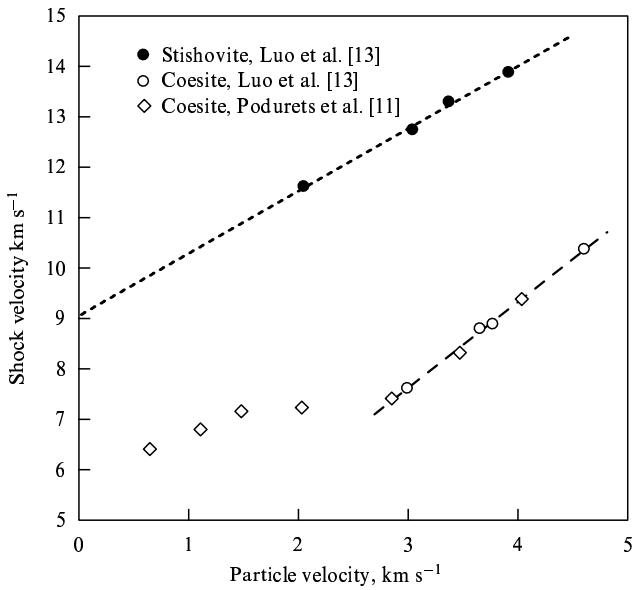

Figure 1. $U_s - u_p$ relationships for stishovite and coesite [11, 13]. Stishovite: U_s (km s^{-1}) $= 9.08 + 1.23\,u_p$, $\rho_0 = (4.31 \pm 0.04)$ g cm^{-3}. Coesite in high-pressure regime (HP): U_s (km s^{-1}) $= 2.52 + 1.70\,u_p$, $\rho_0 = (2.92 \pm 0.03)$ g cm^{-3}.

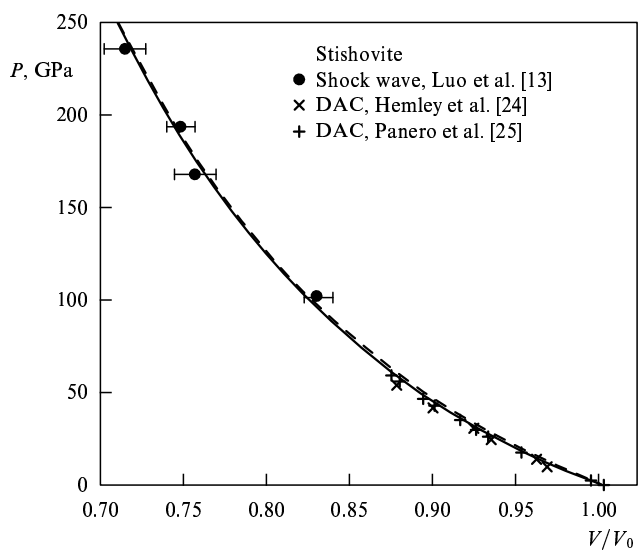

Figure 2. The stishovite $P-V$ Hugoniot [13] with diamond-anvil cell (DAC) data [24, 25]. V_0 is the ambient specific volume of stishovite.

$K_0' = 4.8 \pm 0.2$, comparable to $K_0 = 298 \pm 8$ GPa and $K_0' = 3.98 \pm 0.46$ at 300 K by Hemley et al. [1] The Vinet fit is essentially the same as the curve mapped from $U_s - u_p$ fit. The comparison between the stishovite Hugoniot and DAC results (300 K isotherm) shows that the Hugoniot lies slightly above but very close to the 300 K isotherm at pressures up to 55 GPa, suggesting that the Hugoniot is relatively cold (a rough estimation shows that the temperature at Hugoniot is about 1600 K at 260 GPa). This is consistent with the small compressibility of stishovite. On the contrary, shocked fused quartz is melted at 4500 K and 70 GPa, and α-quartz at 4750 K and 113 GPa as demonstrated by shock temperature measurements [15]. Evidence for post-stishovite phases is not pronounced in the stishovite principal Hugoniot. One possible reason is that the transition is kinetically impeded, although the possibility exists that the minor structural changes of stishovite to post-stishovite cannot be resolved from Hugoniots in $U_s - u_p$ and $P - V$ space. It was proposed that the transition to post-stishovite is exhibited in the fused quartz and quartz principal Hugoniots [19] but it is not evident in the stishovite principal Hugoniot. This could be due to the different shock temperatures along Hugoniots for different silica polymorphs.

Principal Hugoniots centered at four different silica polymorphs have now been obtained. Figure 3 shows the principal Hugoniots for quartz, coesite and stishovite. The fused quartz data are badly scattered and not included. At high pressure, where all the three Hugoniots are in stishovite phase, the internal energy and pressure differences at fixed volume allow estimation of the Grüneisen parameter (γ) of stishovite by finite difference. The Hugoniots in the stishovite regime for quartz and coesite are obtained by fitting to the available data. The Grüneisen parameter for stishovite, $\gamma(V)$, is obtained (see Fig. 4) from quartz–stishovite and coesite–stishovite Hugoniot pairs. The fitting to

$$\gamma = \gamma_0 (V/V_0)^q\,, \quad \text{with} \quad \gamma_0 = 1.35\,, \tag{5}$$

yields $q = 2.6 \pm 0.2$. $\gamma(V)$ obtained from quartz–stishovite pair is slightly different from that from coesite–stishovite

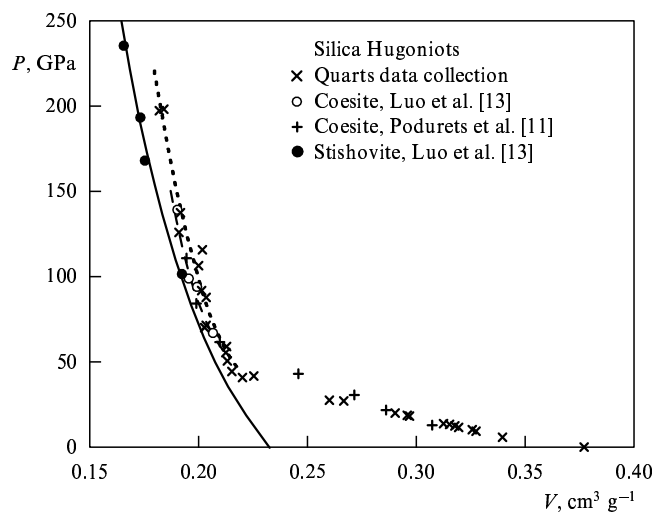

Figure 3. The $P-V$ Hugoniots for quartz [7, 26, 27], coesite [11, 13] and stishovite [13].

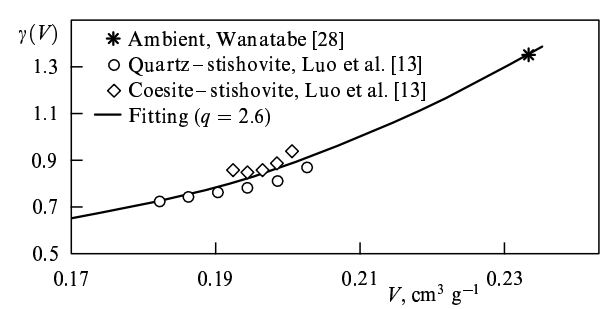

Figure 4. The Grüneisen parameter $\gamma(V)$ for stishovite obtained from the $P-V$ Hugoniots of quartz, coesite and stishovite using Mie–Grüneisen equation of state [13, 28].

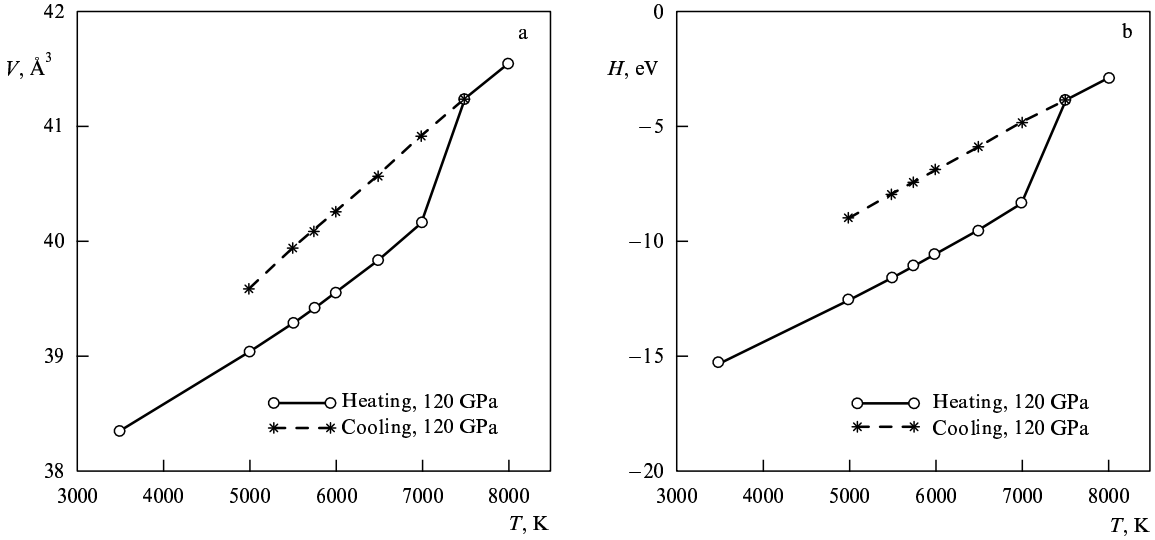

Figure 5. Single-phase simulation of stishovite melting at 120 GPa with molecular dynamics [14]. (a) The unit cell (2 SiO_2 formulae) volume, and (b) the corresponding enthalpy during heating – cooling process.

pair. This could be due to the temperature dependence of γ. The Grüneisen parameter for stishovite at high pressure obtained directly from shock-wave experiments provides an important constraint on thermodynamic calculations.

3. Melting curve of stishovite

Stishovite melting at high pressure has been investigated by using techniques such as shock temperature measurements [15] and diamond-anvil cell experiment [20]. It is still challenging to determine the phase diagram from dynamic and static experiments at high pressures. Several theoretical studies have tackled this issue [14, 21]. The new molecular dynamics (MD) simulations [14] employing Morse-stretch charge equilibrium potential (MS-Q) yielded results in agreement with the shock melting and DAC experiments. In the MD stishovite melting simulation, single- and two-phase simulation methods were utilized. Figure 5 shows an example of single-phase simulation at 120 GPa. The transition

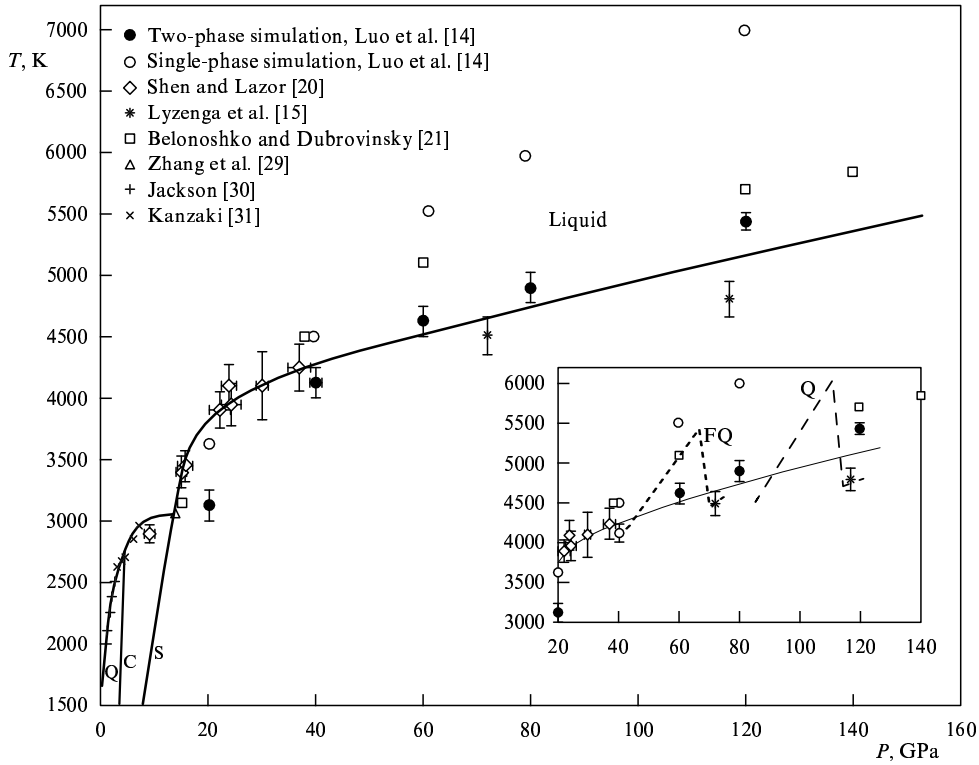

Figure 6. The melting curve of stishovite and silica phase diagram from theoretical and experimental studies [14, 15, 20, 21, 29 – 31]. The solid lines are phase boundaries: Q — quartz; C — coesite; S — stishovite, and FQ — fused quartz. (inset) Dashed lines are shock temperature measurement of shocked fused quartz and quartz [15]. The sharp drop of temperature indicates the melting of stishovite. The portions of Hugoniots above the melting curve (solid line) represent superheated stishovite solid in the shock states.

temperature (7000 K) from solid to liquid stishovite is the melting point (T_m) at 120 GPa from single-phase simulation. The slope of the melting curve (dT_m/dP) can be determined from volume and enthalpy changes using the Clausius–Clapeyron equation. One problem with single-phase melting simulations is the possible superheating of the solid during heating and undercooling of the liquid during cooling due to the kinetics [22] especially at high pressure, which could be reduced by two-phase simulation [23]. The two-phase simulation was conducted by constructing a solid–liquid model by combining the solid and liquid models at the same pressure and temperature from the single-phase simulation. Figure 6 shows the simulation results along with former studies on stishovite melting. At 20 GPa, single-phase simulation appears to be closer to experimental data than the two-phase simulation, possibly due to the simplicity of the force field or the interface effect that is more pronounced at low pressure [14]. At high pressures, the two-phase simulation yielded more accurate results. The melting curve of stishovite is obtained from MD simulation results along with experimental data. The slope of the proposed melting curve is consistent with that computed from single-phase simulation. The MD simulation results are close to the static DAC results at low pressure, and shock wave data at high pressure. This appears to validate the interpretation of superheating of the solid along fused quartz and quartz Hugoniots by Lyzenga et al. [15]. With melting curve of stishovite constrained, the silica phase diagram is extended to the megabar regime.

4. Conclusion

In conclusion, the Hugoniot of stishovite up to 235 GPa was obtained by shocking pure stishovite samples synthesized from multianvil high-pressure press. The coesite Hugoniot in the stishovite regime is in agreement with former study and extended to 140 GPa. The Hugoniots centered at various silica polymorphs have been obtained, from which the Grüneisen parameter for stishovite under compression is experimentally determined. The new molecular dynamics modeling validates the interpretation of shock melting experiments on fused quartz and quartz, and the phase diagram of silica is extended to the megabar regime with sound experimental and theoretical basis.

Acknowledgment. Contribution No. 8856, Division of Geological and Planetary Sciences, California Institute of Technology.

References

1. Hemley R J, Prewitt C T, Kingma K *Rev. Mineral.* **29** 41 (1994)
2. Knittle E, Jeanloz R *Science* **251** 1438 (1991)
3. Song X, Ahrens T J *Geophys. Res. Lett.* **21** 153 (1994)
4. Chao E C T et al. *J. Geophys. Res.* **67** 419 (1962)
5. El Goresy A et al. *Science* **288** 1632 (2000)
6. McQueen R G, Fritz J N, Marsh S P *J. Geophys. Res.* **68** 2319 (1963)
7. Wackerle J *J. Appl. Phys.* **33** 922 (1962)
8. Fowles R *J. Geophys. Res.* **72** 5729 (1970)
9. Ahrens T J, Rosenberg J T, in *Shock Metamorphism of Natural Materials* (Eds B M French, N M Short) (Baltimore: Mono Book Corp., 1968) p. 59
10. Trunin R F *Shock Compression of Condensed Materials* (Cambridge: Cambridge Univ. Press, 1998)
11. Podurets M A et al. *Izv. Akad. Nauk SSSR Fiz. Zemli* **17** 9 (1981) [*Izv. Acad. Sci. USSR Earth Phys.* **17** 9 (1981)]
12. Ito E, Furnish M D, Sandia Report SAND-95-2342 (1995)
13. Luo S-N et al. *Science* (2001), submitted
14. Luo S-N et al. *Earth Planet. Sci. Lett.* (2001), submitted
15. Lyzenga G A, Ahrens T J, Mitchell A C *J. Geophys. Res.* **88** 2431 (1983)
16. Rubie D C *Phase Transitions* **68** 431 (1999)
17. Ahrens T J, in *High Pressure Shock Compression of Solids* (Eds J R Asay, M Shahinpoor) (New York: Springer-Verlag, 1993) pp. 75–114
18. Cohen R E, Gülseren O, Hemley R J *Am. Mineral.* **85** 338 (2000)
19. Akins J (Private communication)
20. Shen G, Lazor P *J. Geophys. Res.* **100** 17699 (1995)
21. Belonoshko A B, Dubrovinsky L S *Geochim. Cosmochim. Acta* **59** 1883 (1995)
22. Allen M P, Tildesley D J *Computer Simulation of Liquids* (Oxford: Clarendon Press, 1987)
23. Strachan A, Çağin T, Goddard W A III *Phys. Rev. B* **60** 15084 (1999)
24. Hemley R J et al. *Solid State Commun.* **114** 527 (2000)
25. Panero W R, Benedetti L R, Jeanloz R *J. Geophys. Res.* (2001), submitted
26. Marsh S P *LASL Shock Hugoniot Data* (Berkeley: Univ. of California Press, 1980)
27. Al'tshuler L V, Trunin R F, Simakov G V *Izv. Akad. Nauk SSSR Fiz. Zemli* (10) 1 (1965)
28. Wanatabe H, in *High-Pressure Research in Geophysics* (Adv. in Earth and Planetary Sci., Vol. 12, Eds S Akimoto, M H Manghnani) (Tokyo: Center for Acad. Publ. Japan, 1982) pp. 441–464
29. Zhang J et al. *J. Geophys. Res.* **98** 19785 (1993)
30. Jackson I *Phys. Earth Planet Int.* **13** 218 (1976)
31. Kanzaki M *J. Am. Ceram. Soc.* **3** 3706 (1990)

PACS numbers: 61.50.Ks, 91.35.Gf, 91.35.Lj

DOI: 10.1070/PU2002v045n04ABEH001159

Minerals of the deep geospheres

D Yu Pushcharovskiĭ

In this report I discuss the composition and structure of the Earth's mantle. Analysis of seismographic maps and the data on the material composition of the mantle shows that the mantle consists of several concentric shells, instead of the common two shells, the upper and the lower. As in the Earth crust, silicates are the predominant substance of the mantle, but structurally the silicates of the mantle differ substantially from those of the crust. More than one hundred tetrahedron complexes in the silicates of the Earth crust are replaced by on more than 20 structure types of this class of minerals in the mantle, and the main difference of these types lies in the transformation of Si-tetrahedrons into Si-octahedrons. In this sense, stishovite may be considered the cornerstone of a new chapter in the history of the crystal chemistry of silicates. New data on the structural transformations of minerals in the deep geospheres suggest that the mineralogical diversity of the deep shells of the mantle is much poorer than that of the Earth's mantle, but nevertheless the mantle mineralogy is not as primitive as it was believed to two to three decades ago.

One of the most intriguing problems of geology in the past decade is related to studies of the composition and structure of the deep shells of the Earth's mantle. Such research in the Earth sciences is of top priority, since more than 90% of matter in the universe is under pressures greater than 1 GPa. The pressure range in the universe is enormous: pressures may vary by more than 60 orders of magnitude. In intergalactic space, there is one atom to more than one cubic centimeter of space, while at the center of neutron stars the state of matter is comparable to the Sun's mass (which is approximately 300